Geometric effects on blackbody radiation

Ariel Reiser and Levi Schächter
Department of Electrical Engineering Technion–Israel Institute of Technology, Haifa 32000, Israel
(Received 26 June 2012; revised manuscript received 4 December 2012; published 1 March 2013)

Planck's formula for blackbody radiation was formulated subject to the assumption that the radiating body is much larger than the emitted wavelength. We demonstrate that thermal radiation exceeding Planck's law may occur in a narrow spectral range when the local radius of curvature is comparable with the wavelength of the emitted radiation. Although locally the spectral enhancement may be of several orders of magnitude, the deviation from the Stefan-Boltzmann law is less than one order of magnitude. The fluctuation-dissipation theorem needs to be employed for adequate assessment of the spectrum in this regime. Several simple examples are presented as well as experimental results demonstrating the effect. For each configuration a geometric form factor needs to be incorporated into Planck's formula in order to properly describe the emitted radiation.

DOI: 10.1103/PhysRevA.87.033801 PACS number(s): 42.50.Ct, 42.50.Nn, 44.40.+a, 05.40.−a

I. INTRODUCTION

From the early days of quantum mechanics via astrophysical measurements to today's nanostructures, blackbody radiation (BBR) is playing a pivotal role in physics. As the emitting bodies were always significantly *larger* than the wavelength of interest, Planck's formula (PF) described adequately the general trend of the emerging radiation and any deviations were described in terms of the so-called emissivity. Conceptually, the emissivity of a passive body was assumed to be always smaller than unity, explicitly assuming that PF provides the upper limit of what a body can emit [1–5]. For quite some time, manufacturing techniques have facilitated the implementation of minute structures of a size *smaller* than or of the same order of magnitude as the radiation wavelength, leading to a new regime of operation in which PF no longer describes adequately the BBR. Assuming PF as an absolute law of physics is a misconception which has been criticized even in textbooks (e.g., Ref. [6], p. 126).

In the remainder of this Introduction, we highlight several of the BBR investigations relevant to the ideas we intend to convey in this study. By no means have we intended this to be a comprehensive review of the field. First we describe in detail Planck's derivation of the radiation within an ideal cavity. This we do in some detail in order to emphasize the source of its limitations. In addition, we do not distinguish here between BBR that is generally attributed to closed structures (cavities) and thermal radiation (TR) that describes radiation emitted by a body of nonzero temperature into free-space.

Planck's [7] original argument consists of three steps. In the *first* one he considered an ensemble of oscillators in thermal equilibrium and he established, using the classical Maxwell-Boltzmann statistics and using elementary quantum notions, that the energy of a system consisting of N_{osc} oscillators at a given frequency is $\mathcal{E} = N_{\mathrm{osc}}\Theta(T,\omega)$, wherein $\Theta(T,\omega) = \hbar\omega[\exp(\hbar\omega/k_B T) - 1]^{-1}$ denotes the mean energy of a single oscillator.

The *second* step was to count the number of modes ($\Delta N_{\mathrm{cavity}}$) within a frequency interval—that is to say, the density of states (DOS)—in a cavity of *perfectly reflecting* walls of volume V_{cavity}. Subject to the tacit assumption that the wavelength is much *shorter* than the typical dimension of the cavity $\sqrt[3]{V_{\mathrm{cavity}}}$, the number of modes in a range of frequencies $\Delta\omega$ starting at ω is

$$\Delta N_{\mathrm{cavity}} = V_{\mathrm{cavity}} \frac{\omega^2 \Delta\omega}{\pi^2 c^3}, \tag{1}$$

accounting for both possible polarizations.

His *third* step was to correlate the statistics of oscillators with the DOS in a cavity, which is a delicate matter. Essentially, there must be an equilibrium between the radiation in *vacuum* and its source in *matter*, which comes about when a wave impinging upon the walls is absorbed, causing another wave to be radiated so that the walls can be conceived as *perfect reflectors*; in other words, $N_{\mathrm{osc}} = \Delta N_{\mathrm{cavity}}$. With this assumption, the energy spectral density ($u = U/\Delta\omega$) is

$$\frac{u}{V_{\mathrm{cavity}}} = \frac{\omega^2}{\pi^2 c^3} \frac{\hbar\omega}{\exp(\hbar\omega/k_B T) - 1}. \tag{2}$$

What is unique about Planck's formula is the fact that the right-hand side is independent of the geometry or the properties of the body. As such, many consider it as a fundamental law and in this regard it as an upper limit to what a body can emit.

In the framework of Planck's formulation, there is a distinction between the number of oscillations N_{osc} which is derived from *geometrical* considerations, and their mean energy Θ which is derived from *statistical* considerations and is therefore independent of the geometry of the problem. While Θ is correct because there is a large number of possible energy states in a harmonic oscillator, and $\mathcal{E} = N_{\mathrm{osc}}\Theta$ is almost always correct since the number of atoms (microscopic emitters) is very large, one can question the validity of the calculation of the DOS. The latter is a good approximation only for a cavity of "infinite" volume in respect to the wavelengths of interest. A formal mathematical proof for the validity of (2) given this assumption is given by Courant and Hilbert [8].

Planck himself, when determining the thermal energy density within a cavity, states that "No matter how small the frequency interval $\Delta\nu$ may be assumed to be, we can nevertheless choose l sufficiently great," where l is the cavity's dimension [[7], p. 273]. Later, Rytov [9], Eq. (5.5) indicates that Planck's law is applicable only if $1 \gg \Delta\lambda/\lambda \gg (\lambda/l)^3$, where $\Delta\lambda = \lambda\Delta\nu/\nu$ is the frequency interval measured in wavelengths, "thus, the conditions for the validity of PF are first, a not too large mono-chromaticity of the spectral interval, and second, sufficiently large dimensions of the volume under study in comparison to λ."

Moreover, it is important to realize that it is customary to derive the Stefan-Boltzmann (SB) law from the integration of PF, which also subjects it to the requirements mentioned above. One may claim that the SB law actually preceded Planck's law and is thus a more fundamental law. Yet, it is derived from ray optics, which assumes that the wavelengths are much smaller than the dimensions of the bodies *and from their spatial variations* [[7], Sec. 94]. Consequently, this law too is not immune to criticism.

As already indicated, Planck derived his formula based on geometrical considerations and explicitly states that the typical geometric parameters are much larger than the wavelength. Einstein arrives at the same formula from a totally different perspective. In his 1917 paper [10], he introduced a new concept of probability rates of spontaneous emission, stimulated absorption, and stimulated emission; then he looked for the particular radiation density for which the exchange of energy between radiation and molecules will not disturb the state of equilibrium (which is quantified by the Maxwell-Boltzmann distribution). He uses Wien's displacement law in order to describe the radiation density. The latter was formulated subject to the assumption of ray bundles [[7], Sec. 112]; therefore, Einstein's derivation is limited to structures large enough for ray theory to be correct.

Shortly after Planck's publication, Weyl published a series of papers studying the scalar wave equation's eigenvalue distribution. A summary of his work is found in Ref. [11]. Although this is presented as a pure mathematical question, it is closely related to the question of the evaluation of high-order correction terms to Planck's formula that should not be neglected for large but finite-sized cavities. This topic was further elaborated [8,12–14] and specifically treated for the electromagnetic vector wave equations $\nabla^2\vec{u} + \lambda\vec{u} = 0$ by Baltes and Hilf, who summarized their work in a textbook [15]. The epitome of this research is that the correction to Planck's derivation (2) due to the finite size of the cavity (which has perfectly reflecting walls) is given by [[15], Chap. VII, Sec.4]:

$$\frac{\Delta N}{\Delta\omega} = V_{\text{cavity}}\frac{\omega^2}{\pi^2 c^3} - \frac{\Lambda}{2\pi c} + \cdots, \tag{3}$$

wherein the correction term is $\Lambda_{\text{cuboid}} = a_x + a_y + a_z$, $\Lambda_{\text{sphere}} = 4R/3$, or $\Lambda_{\text{cylinder}} = \pi R + 4H/3$, for the specified simple geometries of the cavity. The Stefan-Boltzmann law of the total energy (in Joules) is also corrected to read

$$E(T) = a_0 V_{\text{cavity}} T^4 + a_2 \Lambda T^2 + a_3 T + a_4/\Lambda; \tag{4}$$

here $a_0 = 4\sigma/c$, $a_3 = k_B/2$, and a_2,a_4 are shape-dependent constants. In the case of a cube these corrections (with [15], Eq. (V.68), $a_2 = -\pi k_B^2/12\hbar c$, $a_4 = -0.2751\hbar c$) were numerically computed and compared to the rigorous sum $E(T) = \sum_{i=1}^{\infty} g_i \frac{\hbar\omega_i}{e^{\hbar\omega_i/kT}-1}$ and were shown to be valid (up to 1% error) for medium-sized cavities. For smaller cavities or for lower temperatures, these expansions fail. For example, at 300 K Eq. (4) is valid for a cube down to 10 μm size. These corrections to the classical formulas have even recently been experimentally verified and reported [16].

From Eq. (3) we learn that different geometries have different spectral densities of energy, which is due to the different mode distribution. This diversity of the spectral behavior of cavities stands in direct contradiction to the statement of classical thermodynamics that all cavities hold the exact same spectral density of energy—see Ref. [[17], p. 380].

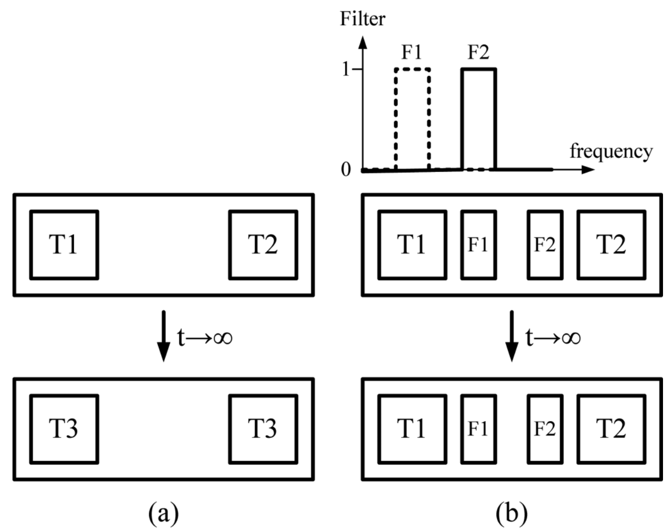

FIG. 1. Blackbodies reach thermal equilibrium only if radiation is allowed to pass from one body to the second.

In order to clarify where the classical logic fails, let us first consider the case of two ideal blackbodies placed inside an enclosure, which at a given instant are at different temperatures. After a period of time they will be at thermal equilibrium as in Fig. 1(a). However, if we insert filters of incongruent frequencies, no radiation will pass from the first body to the second, nor in the opposite direction, and the temperatures will not vary. This situation is sketched in Fig. 1(b). If the filters have some congruency than thermal equilibrium will be reached, and the larger the frequency overlap, the more quickly this will happen. Yet the conclusion $u_1(\omega) = u_2(\omega)$ will be true only in this interval of overlapping frequencies, whereas the radiation may be different at other frequencies. Now, let us take two different cavities at identical temperature which are connected through a hole. The shape of the cavity does not allow all modes to propagate inside. This implies that even modes of frequencies high enough to pass through the hole will not necessarily pass from one cavity into the second cavity. Hence, the second cavity will not absorb these frequencies and therefore will not radiate them. This argument limits the validity of the condition of detailed balance to frequencies which can be supported by both cavities.

Essentially, all the work done on geometry-dependent corrections to Planck's law is based on the claim that the geometry acts as a weak filter, enabling most modes to pass, but not all; thus loosening the condition of detailed balance and enabling bodies of different geometries to emit a different spectrum.

Up to this point we have discussed the evaluation of thermal energy within an enclosure. However, from the practical perspective, at least as important is the question of energy radiated by a body at temperature T from its surface to the surrounding environment. In such a case the classical equation for the power radiated per unit area from the surface of a body whose absorption and emission are independent of direction (isotropical) and of polarization is given by [17]

$$P_e(\omega) = a(\omega)\, c\, \bar{u}(\omega)\tfrac{1}{4}. \tag{5}$$

Here $a(\omega)$is the absorbance, which is a frequency-dependent factor varying from zero to 1, multiplied by Planck's relation for the spatial spectral density of energy $\bar{u}(\omega) = u(\omega)/V_{\text{cavity}}$, by the energy velocity of plane waves in vacuum (c), and by $1/4$, which accounts for the fact that there are standing waves in the cavity. Here we are interested in the energy flux of the waves propagating in one direction (both polarizations). Consequently, it is evident that since Eq. (2) is derived for a large cavity, the relation in Eq. (5) is valid only for bodies that are large compared to the wavelength of interest. When studying surfaces with local radius of curvature (or cavities) of the same scale as the wavelength, the fluctuation-dissipation theorem (FDT) must be employed—see Callen and Welton [18], Landau and Lifshitz [19], and Rytov [20]. This will be discussed in detail subsequently.

In this study we demonstrate that when the geometrical size is not much larger than the wavelength of interest a geometric form factor must be included in Eq. (2). Several quasianalytic examples are presented and we show that it is possible to have spectral enhancement in some limited interval such that the radiation emitted exceeds the value predicted by PF at the same temperature.

Various research has been conducted with the motivation of controlling thermal emission. This can be roughly classified into three categories: field coherency, thermal photovoltaic systems (TPVs), and enhanced thermal spectrum. The first category deals with the *coherence* of the electromagnetic wave, which is the correlation between the fields in two different locations at two different times. Assuming that the process of fluctuation of the field is stationary, the coherence is a function of $t_2 - t_1$ and is written as $\Gamma(\vec{r}_1,\vec{r}_2,t_2 - t_1) = \langle E(\vec{r}_1,t_1)E^*(\vec{r}_2,t_2)\rangle$. This topic was thoroughly studied by Mandel and Wolf [21] and Wolf and James [22]. They showed that although classically a thermal source is assumed to be uncorrelated, both spatially and temporally, yet a scalar field does possess a spatial coherence length of $\lambda/2$. This was later generalized for vector fields [23,24]. In a series of papers [25–29] well summarized in [30], Greffet and co-workers worked to optimize the thermal spectrum by harnessing the contribution of evanescent waves near the surface, utilizing knowledge of the spatial coherency of the fields together with the FDT. Further studies using evanescent waves and gratings can be found in Refs. [31–37].

The second category of research deals with TPVs. A controllable spectral radiation is important in TPV systems in order to achieve higher efficiencies from solar cells. Our perception of a good system [38] is similar to that of Rephaeli and Fan [39,40], that is, a system containing a medium which is structured on one side to be an optimal absorber of the solar spectrum and on the other side to be an optimal thermal emitter towards a PV cell. Rephaeli and Fan structured a tungsten slab into pyramids in order to achieve high absorptivity of the sun's spectrum, and devised a plain tungsten slab followed by Si and SiO_2 plates in order to suppress sub-band-gap and super-band-gap radiation, which, over time, hinder the detector. Many others have used photonic crystals in order to achieve a similar goal; for an example see Refs. [41,42]. Other suggestions for controlling the thermal spectrum include selective heating of cells in a photonic lattice [43], metamaterials [44], or semitransparent semiconductor plates [5,45].

The possibility of enhanced BBR or TR spectra in the far field is the topic of discussion in the third category of research. It was first raised in the framework of separate experiments on metallic photonic crystals [46–48]. However, it was ruled out as violating the second law of thermodynamics [49]. As a consequence the authors of the first study acknowledged the possibility that the measurements were not taken at thermal equilibrium [50]. This exchange initiated a study by Luo *et al.* [51] to determine the thermal emission of photonic crystals. They demonstrated that the thermal emissivity spectrum equals the absorption spectrum, and concluded that "the photonic crystal is not expected to emit more than that from a blackbody," thus suggesting the impossibility of an enhanced BBR spectrum. However, Bohren and Huffman [6] have previously shown that the absorption area of a small body is greater than its geometrical area; therefore the fact that the emissivity equals the absorptivity actually leads to the opposite conclusion—that we actually do expect a greater emittance than that established by PF.

The same reasoning also holds when we examine Han's [3] analytical proof that Kirchhoff's law is true for photonic crystals; that is to say, even when the structural components are comparable in size to the wavelength, as long as they are periodic and the overall dimension is much larger than the wavelength, then the emissivity equals the absorptivity. It is important to notice that Han was careful not to claim that Kirchhoff's law is true for a small body, nor at a short distance from the surface where evanescent waves may be significant. Another study regarding the thermal emission of photonic crystals was carried out by Chow [2] and is often referred to as a proof that a body in thermodynamic equilibrium cannot radiate into free space more than the value predicted by PF. We discuss Chow's study in Sec. IV.

The major question which we raise is that of the validity of an enhanced spectrum. In this study we endeavor to clarify the limits of PF: (i) How does the blackbody radiation energy change within a cavity as the geometrical dimensions change? (ii) How does the thermal radiation flux change as the dimensions of an open surface change?

In Sec. II we address the question of the variation of the blackbody radiation energy within a cavity as the geometrical dimensions change. We study a closed cavity and give simple examples demonstrating the possibility of violating "Planck's law." We find that when the dimensions of the cavity are of the same order of magnitude as the wavelength there is a substantial deviation from PF. As a consequence the SB law must be modified, and we obtain an analytical approximation of the necessary modification.

In Sec. III we employ Callen and Welton's fluctuation-dissipation theorem which, in the case of a dipole oscillating in free space, can be shown to be identical with PF. By examining simple configurations we show that the energy density in a narrow wavelength range may substantially exceed the value predicted by PF.

In Sec. IV we address the question of the change in the thermal radiation flux as the dimensions of an open surface vary. We introduce Rytov's formulation for the radiated thermal energy from the surfaces of bodies. Then we establish the characteristics of the thermal radiation emitted when the dimensions of the blackbody are comparable to or smaller than the typical wavelength. We find that an enhanced spectrum can be obtained in the far-field radiation flux.

In Sec. V we conclude with a discussion of the possibility of controlling thermal radiation by utilizing devices with geometrical features which will enhance the spectrum at predetermined wavelengths. A simple experiment supporting the theoretical predictions is presented.

II. RADIATION IN A CLOSED CAVITY

Our goal in this section is to establish the spectral density with special emphasis on the geometry of the cavity. Planck's BBR spectrum, as it is reflected in (2), is linearly dependent on the volume of the cavity; therefore we examine various cavities all of the *same volume*, but of different shapes. This is done by taking a cube and flattening it out into a thin film or thinning it into a rod. In both cases, the base is kept square, $a_x = a_y$. We pursue the following procedure for calculating the exact energy in a cavity. First we scan over all relevant $\{n_x,n_y,n_z\}$ sets and calculate the resonant frequencies $f_{\{n\}}$ according to

$$f_{\{n\}} = \frac{c}{2}\sqrt{\left(\frac{n_x}{a_x}\right)^2 + \left(\frac{n_y}{a_y}\right)^2 + \left(\frac{n_z}{a_z}\right)^2}. \tag{6}$$

Next we sort these frequencies in ascending order. This readily gives the number of modes up to a frequency f:

$$N(f) = \sum_{n_x,n_y,n_z | f_{\{n\}} \leqslant f} 1. \tag{7}$$

Assigning the mean energy of each resonant frequency (oscillator) $\Theta_{\{n\}} = hf_{\{n\}}/(e^{hf_{\{n\}}/kT} - 1)$ we can establish the total energy of the ensemble (in Joules) as

$$U(T,f) = \sum_{n_x,n_y,n_z | f_{\{n\}} \leqslant f} \Theta_{\{n\}}(T,f_{\{n\}}). \tag{8}$$

For practical purposes we need to evaluate the spectral energy density and compare it to PF. With this in mind, we split the information regarding the resonant frequencies $f_{\{n\}}$ into two: a list of different resonant frequencies and the corresponding degeneracy of modes at each resonance. Based on this notation we may now infer the degeneracy of modes $\Delta N(f) = \sum_{n_x,n_y,n_z | f \leqslant f_{\{n\}} \leqslant f+\Delta f} 1$, where Δf is taken from one resonant frequency to the next, starting from the first resonance, below which there is no radiation energy, and continuing *ad infinitum*. Explicitly, the energy density (J/Hz) is

$$u(T,f) = \Theta(T,f)\,\frac{\Delta N(f)}{\Delta f}. \tag{9}$$

We establish the accuracy of this procedure by comparing the integral of (9) with (8) and confirming that the error is nothing but computational inaccuracies. According to PF, 99.99% of the energy at 300 K is under 98.9 THz; we therefore extend our observations up to $f_{\max} = 100$ THz in order to obtain exact results and compare them to the theoretical total energy of our volume, which, according to the Stefan-Boltzmann law is

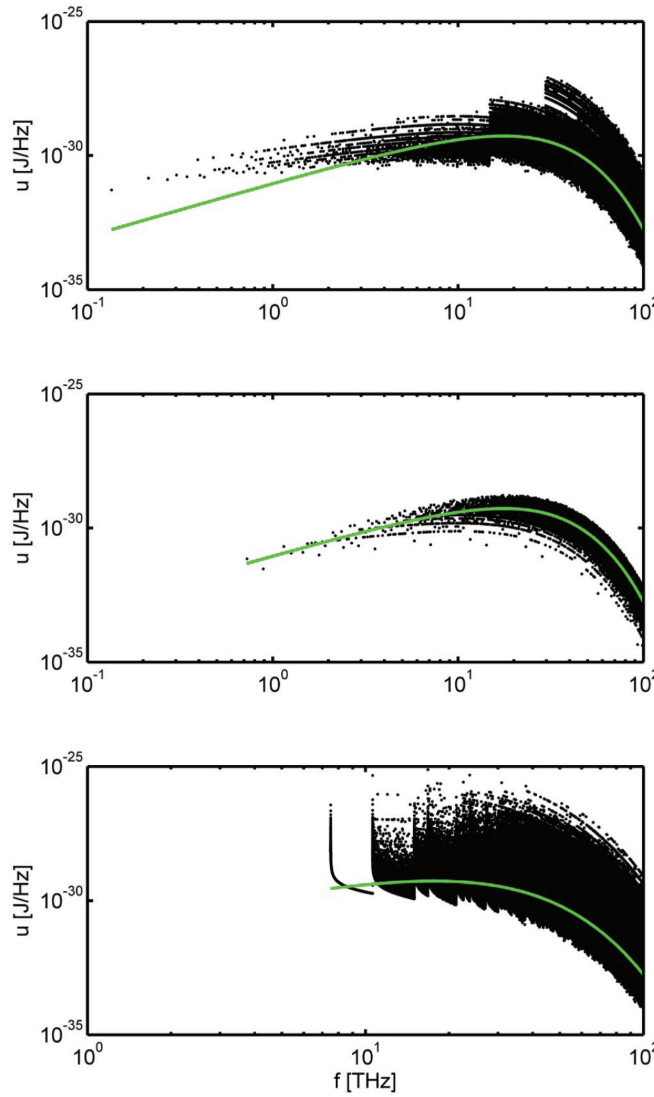

FIG. 2. (Color online) Energy density for a film (top), cube (center), and rod (bottom) of equal volume (0.025 mm^3); the rod and film have a similar surface area of 18 mm^2; $T = 300$ K. The PF result is plotted for comparison. Each dot represents a value which is exact for a specific frequency of oscillation.

$U_0 = (4\sigma V/c)T^4 = 1.531 \times 10^{-16}$ J, where SB's constant is $\sigma = 5.67 \times 10^{-8}$ W m^{-2} K^{-4}.

For illustrating the energy density $u(T,f)$ we plot points representing the energies at specific frequencies, as illustrated in Fig. 2. We already mentioned Rytov's comments that PF is applicable only if the monochromaticity is not too sharp. Consequently, the choice of the smallest possible frequency interval is one obvious reason for the discrepancy between the estimate used to describe the ensemble and PF. It will be shown subsequently that smoothing the mode counting does not overcome the discrepancy.

For practical assessment, we are interested in forming a curve which will convey the trend of the data points in Fig. 2 and allow us to make a quantitative comparison of different geometries. A straightforward solution would be to average the energy over small frequency intervals. We do this for every M (=100) points, and use Δf as a weight for each

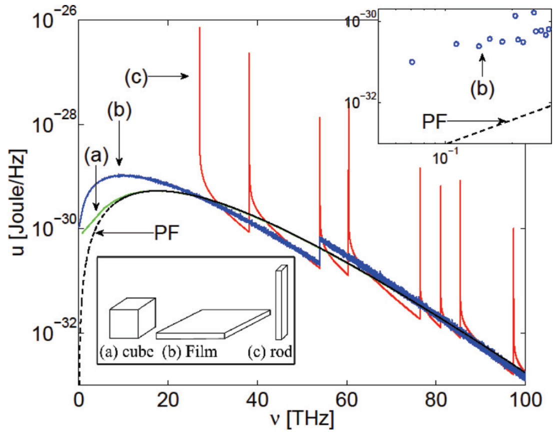

FIG. 3. (Color online) Comparison of energy density within various cavities. Rectangular cavities of equal volume (0.025 mm^3) are employed for assessing the energy density spectrum at extreme geometries: the rod (c) and film (b) have a similar surface area of 18 mm^2 (bottom left inset); $T = 300$ K. The PF result is plotted for comparison (dotted). For a thin rod, near cutoffs, the spectrum in a closed cavity may be orders of magnitude greater than in the case of a cube of the same volume (a). Top right inset: Energy levels of the film at low frequencies, depicting the first modes of oscillation which are distinct and do not form a continuum; thus conceptually approximating the DOS to a continum is problematic.

point, resulting in the average and variance

$$\langle u\rangle = \frac{1}{\sum_{i=1}^{M}\Delta f_i}\sum_{i=1}^{M}\Delta f_i u_i,$$
$$\Delta u^2 = \frac{1}{\sum_{i=1}^{M}\Delta f_i}\sum_{i=1}^{M}\Delta f_i\,(u_i-\langle u\rangle)^2 \tag{10}$$

In Fig. 3 we compare the energy density for a film, a rod, and a cube. The various cavities store zero energy below the first mode of oscillation, and a certain amount of radiation at frequencies above that, when the first few modes, for which one cannot ascribe a density of states (DOS) are ignored—see the top-right inset of Fig. 3. As these are low frequencies, there is a great deviation from PF, which conceptually is not valid in this range. More interesting is the deviation at higher frequencies, in which PF is supposedly exact. While the cube (which has relatively large dimensions) is very close to PF, the rod and the film are not. The smaller the base of the rod or the height of the film, the more extreme are the deviations from PF, and local enhancement of the energy spectrum may be greater than two orders of magnitude. This is one of the important results of the present study. It is interesting to compare the results of the film to the results of the discussion on heat transfer between two infinite planes which are closely spaced in Ref. [52]. The latter is a two-dimensional version of the former; hence the similarity.

Once the energy spectrum is analyzed, we can proceed to investigate the total energy. In Fig. 4 (top) we plot the total energy stored in two cavities of different volumes ($V =$ 0.025 and 0.01 mm^3) as a function of the geometric parameter $a_z^2/a_x a_y$, at a given temperature (300 K). The continuous (blue) curve clearly reveals that for relatively modest deviations from a cube, the SB law (horizontal dashed black line) is an excellent

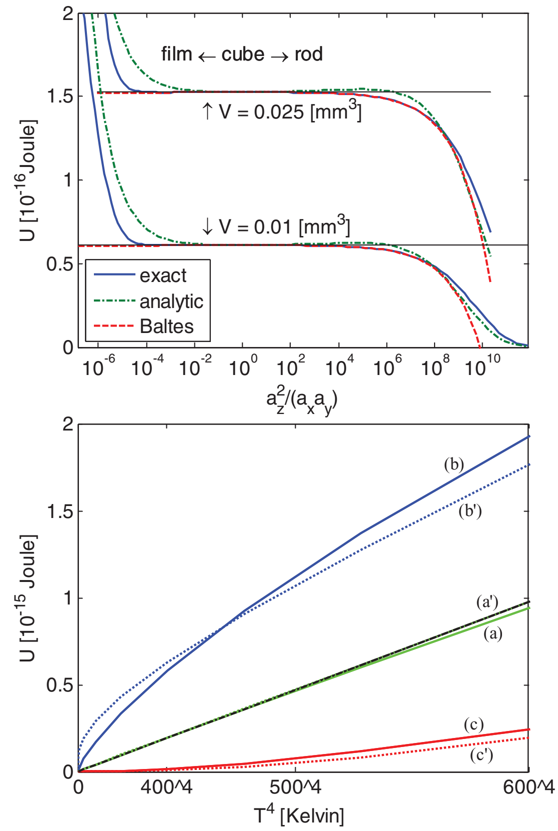

FIG. 4. (Color online) Analytical modification of the Stefan-Boltzmann law: Top: SB law (dotted) is constant for all geometries of equal volume. The analytic expression (2.8) (dash-dotted) is compared with the calculated total energy for various geometries at $T = 300$ K (solid), and to the expression developed by Baltes and Hilf (4) (dotted), over the various geometries with two constant volumes: 0.01 mm^3 and 0.025 mm^3. The result of the SB law is given for reference (dashed). We see that the analytic expression has a better fit for extreme geometries where Baltes and Hilf's expression fails. Bottom: Total energy as a function of the temperature; $V = 0.01$ mm^3. The exact calculations are plotted as solid lines and the analytic expression (11) is plotted as dotted lines for the cube (a),(a'), film (b), (b'), and rod (c),(c'). The surface area of the film and rod equals 18 mm^2. The result of the SB law is given for comparison (dot-dashed).

approximation. Non-negligible deviations occur for a very thin film ($a_z^2/a_x a_y \ll 1$) or a very long rod ($a_z^2/a_x a_y \gg 1$). However, while in the energy spectrum we calculated in a narrow frequency range an enhancement of several orders of magnitude above the values predicted by PF, the total energy deviation (from the SB law) is by far more modest, reaching values which are less than one order of magnitude different at extreme geometries.

For the case of a long and thin rod we may readily comprehend the behavior since as the rod gets longer, the transverse dimension becomes shorter, and as result, the first resonant frequency gets higher, until it exceeds $f_{\max}$. At this stage there is practically no energy in the cavity. This happens in mode (011) or (101) when $a_x = a_y = c/2f_{\max}$, leading to $a_z = V_{\text{cavity}}/(c/2f_{\max})^2$, which in our case corresponds to $a_z^2/a_x a_y = 5.5\times10^{13}$.

In the thin-film case a divergence occurs as a consequence of the "infinite" modes at low frequencies. To some extent, this phenomenon resembles the infrared catastrophe, when electrons are scattered by protons and photons are emitted with an energy spectrum which diverges at low frequencies. The problem is usually dealt with [53,54] by claiming that since every experimental apparatus has a finite resolution ΔE, one does not need to count photons that cannot be detected, $\hbar\omega < \Delta E$. Similarly, in our case, if we stop the mode counting below a certain frequency, our energy will not diverge.

A different perspective may be reached when examining the energy as a function of temperature. In the curves illustrated in Fig. 4 (bottom) we limit ourselves to 600 K since as the temperature increases, one must calculate the energy up to higher frequencies, which results in longer calculations without any added value to the present study. Figure 4 (bottom) shows the energy as a function of the temperature (T^4) for three geometries, a thin film, a cube and a long rod, for the same volume. Three trends are evident: (i) The cube at any temperature follows the SB law. (ii) The T^4 scaling is asymptotically approached by both the film and the rod for high temperatures but systematically the energy in the case of the thin film is higher than that of a cubical cavity of the same volume. For the rod, the stored energy is lower. (iii) In both cases the change in the stored energy compared to the SB result is less than one order of magnitude.

Based on the results of a series of simulations similar to these described above, we were able to construct an analytic function that approximates reasonably well the simulation results in a broad range of the four variables frequency, temperature, and volume and surface of the cavity. This function has several main features: (i) It converges to PF for a cube $(1/V)(S/6)^{3/2} = 1$, (ii) it increases as the square root of the temperature, and (iii) it vanishes below a cutoff frequency. Consequently, it has the following form:

$$\begin{aligned} u_{\text{app}}(T,f,V,S) &= \left\{u_{\text{Planck}}(T,f,V) + \kappa\sqrt{T}\left[\frac{1}{V}\left(\frac{S}{6}\right)^{3/2} - 1\right] h\exp\left(-\frac{hf}{k_B T}\right)\right\} s\,(f - f_{\text{cutoff}}), \\ U_{\text{app}}(T,V,S) &= \int_{f_{\text{cutoff}}}^{\infty} df \left\{u_{\text{Planck}}(T,f,V) + \kappa\sqrt{T}\left[\frac{1}{V}\left(\frac{S}{6}\right)^{3/2} - 1\right] h\exp\left(-\frac{hf}{k_B T}\right)\right\}, \end{aligned} \tag{11}$$

wherein $s(x)$ is the step function, the cutoff frequency is the lower of the (011) and (110) modes, u_{Planck} is given by (8), the empirical coefficient κ has units of $1/\sqrt{\text{K}}$, V is the volume of the cavity, and S is the surface of the body. A rough optimization shows that $\kappa = 7.5$ provides a good approximation. Defining the error as $100\sqrt{\frac{1}{N}\sum_{i=1}^{N}\left(\frac{U_i - U_{\text{app},i}}{U_i}\right)^2}$ we found 1.96% error if the volume is 0.01 mm^3 or 0.7% for a volume of 0.025 mm^3. Taking $\kappa = 7.5$ one obtains an estimate of the total energy as a function of body geometry and an estimate of the total energy as a function of temperature. These are plotted as the curves labeled (a) and (b) in Figs. 4. Both estimates are close to the calculated values, and therefore U_{app} may be conceived as a good correction to the Stefan-Boltzmann law. For large cavities the integration starts practically from zero, and amounts to

$$U_{\text{app}} = (4\sigma V/c)\,T^4 + \left\{\left[\left(\frac{S}{6}\right)^{3/2}\frac{1}{V} - 1\right]\kappa k_B\right\} T^{3/2} \tag{12}$$

in which case the second element is negligible, and this expression reduces to the well-known Stefan-Boltzmann relation.

Finally, the dashed (red) line in Fig. 4 (top) reveals the energy according to Baltes and Hilf's correction [15]. Clearly, for the long-rod configuration, their analytic estimate fits our exact calculations and approximate expression well, but for very thin films, their expression fails to describe the exact calculation as well as our approximation.

To summarize this section, we described the method used to count the number of oscillation modes within a cavity. We explored the limits of accuracy of Planck's law and of the Stefan-Boltzmann law; explicitly, we showed that an enhanced BBR may be achieved in some frequency intervals. While in a narrow range the spectral enhancement can be of a few orders of magnitude, the overall energy does not change dramatically.

III. FLUCTUATION-DISSIPATION THEOREM AND BBR

Contrary to Planck's approach where the BBR spectrum was considered from the perspective of the *electromagnetic field*, in this section we investigate this spectrum from the perspective of the *oscillating electrons* in the matter surrounding the cavity. Because there is thermodynamic equilibrium between the radiation and the surrounding matter in a closed structure, the two approaches are obviously equivalent, and the reason we consider this approach is associated with the generalization to open structures, which is rather natural when considering the process from the electron's perspective.

Essential to this approach is the fluctuation dissipation theorem developed by Callen and Welton [18]. Originally, the motivation was to find a relation between the microscopic spontaneous motion of electrons generating heat via scattering from atoms and the macroscopic resistance to forced motion, which physically arises from similar collisions. Let us highlight the basic concepts of the FDT: A system is *dissipative* if it is capable of absorbing radiation when subjected to a steady-state perturbation. We denote by $V(t)$ the function of time which measures the magnitude of the external force applied on the system, and by $Q(x,p)$ the function of coordinates and momenta which measures the response of the system to the external force. We now define the *generalized impedance* of a linear system to be the ratio between the applied force and the change in time which it causes in the system: $Z = V/\dot{Q}$. The resistance of the system to the perturbation is therefore $R(\omega) = \mathrm{Re}[Z(\omega)]$. A system on which no external force is imposed fluctuates nonetheless. This fluctuation is associated with a spontaneous fluctuating force V, which has a zero mean ($\langle V\rangle = 0$) but a nonzero variance $\langle V^2\rangle \neq 0$. Using fluctuations between the quantum energy levels of a system, Callen and Welton showed that it is possible to evaluate the mean square of the fluctuating force acting on the system through the system's resistance to applied external forces:

$$\langle V^2\rangle = \frac{2}{\pi}\int_0^\infty d\omega R(\omega)\,\mathcal{E}(\omega,T). \tag{13}$$

Here $\mathcal{E}(\omega,T) = \hbar\omega[\frac{1}{2} + \frac{1}{\exp(\hbar\omega/k_BT)-1}]$ is the mean energy of a harmonic oscillator with an added ground-state energy $\hbar\omega/2$ representing the contribution of the vacuum fluctuations, and it will be ignored in what follows.

At first sight, one may wonder what this result has to do with BBR. To address this question one needs to bear in mind that due to the *equilibrium* condition between the radiation absorbed by the lossy material and the radiation generated due to the thermal motion of the electrons, from the latter's perspective we may consider in zero order the *radiation resistance* of an electric dipole in vacuum. Consider a dipole $p = ed$ of charge e and displacement d in free space, pointing in the z direction; its average energy flux far away from the source is

$$S_r = \frac{1}{2\mu_0 c}\left(\frac{\omega}{c}\right)^4\left(\frac{p}{4\pi\varepsilon_0}\right)^2\frac{\sin^2\theta}{r^2} \tag{14}$$

and the total emitted power reads

$$\begin{aligned} P_{\mathrm{FS}} &= r^2\int_0^{2\pi} d\varphi\int_0^\pi d\theta\sin\theta\, S_r = \frac{\eta_0}{12\pi}(\omega p)^2\left(\frac{\omega}{c}\right)^2 \\ &= \frac{\eta_0}{12\pi}(Id)^2\left(\frac{\omega}{c}\right)^2, \end{aligned} \tag{15}$$

where we emphasized that we are dealing with a free-space problem by adding the FS subscript, and where we denoted the current associated with the oscillation of the dipole by $I = q\omega = p\omega/d$. Thus the free-space radiation resistance is

$$R_{\mathrm{FS}} = \frac{P_{\mathrm{FS}}}{I^2/2} = \frac{\eta_0}{6\pi}(d)^2\left(\frac{\omega}{c}\right)^2. \tag{16}$$

Subject to this observation, the mean square of the fluctuating electric field in the vicinity of the dipole is, using (13) and writing $V = E_z d$,

$$\langle E_z^2\rangle = \eta_0\frac{1}{3\pi^2c^2}\int_0^\infty d\omega\omega^2\mathcal{E}(\omega,T). \tag{17}$$

Now, the relevance of the FDT to BBR is straightforward since the energy density (J/m^3) near three fluctuating dipoles (p_x,p_y,p_z)at each location sums up to

$$\begin{aligned} \varepsilon_0\langle E^2\rangle &= \varepsilon_0(\langle E_x^2\rangle + \langle E_y^2\rangle + \langle E_z^2\rangle) = \varepsilon_0(3\langle E_z^2\rangle) \\ &= \frac{1}{\pi^2c^3}\int_0^\infty d\omega\omega^2\mathcal{E}(\omega,T). \end{aligned} \tag{18}$$

Ignoring the ground-state contribution ($\hbar\omega/2$), this expression is identical to Planck's BBR formula. However, we again wish to emphasize that the focus of this approach is the individual oscillating electron (dipole). Having this approach in mind, we realize that if the individual dipoles representing the thermal atoms experience a radiation resistance greater than that of free space, the overall emitted energy may exceed that predicted by PF. Explicitly, we can conceive geometries such that the power emitted will be represented by a form factor $F(\omega)$ that multiplies the free-space value:

$$\begin{aligned} &P = P_{\mathrm{FS}}F(\omega) \Rightarrow R = \frac{P_{\mathrm{FS}}F(\omega)}{I^2/2} = R_{\mathrm{FS}}F(\omega) \\ &\Rightarrow \varepsilon_0\langle E^2\rangle = \frac{1}{\pi^2c^3}\int_0^\infty d\omega\omega^2\mathcal{E}(\omega,T)\,F(\omega). \end{aligned} \tag{19}$$

Thus, the FDT enables a relatively simple estimate of the geometric effect if the size is of the order of the wavelength. In fact, the power emitted by the same dipole located at the center ($r = 0$) of a dielectric layer medium ($R_{\mathrm{int}} \leqslant r \leqslant R_{\mathrm{ext}}$) may exceed, near resonance, the free-space value by almost one order of magnitude—see Fig. 5, which shows the emitted BBR spectral density for a SiC layer; the dielectric coefficient is illustrated in the inset.

Two additional simple examples warrant consideration: (i) a dipole at a height h above an ideally conducting plane, and (ii) a dipole oscillating in a partially open structure

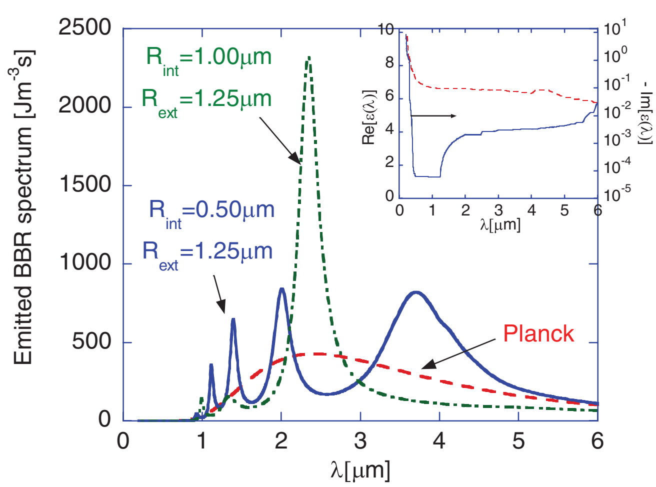

FIG. 5. (Color online) The radiation emitted by dipoles located in the center of a SiC dielectric layer for $R_{\mathrm{int}} = 0.5\ \mu$m, $R_{\mathrm{ext}} = 1.25\ \mu$m (solid) and for $R_{\mathrm{int}} = 1.0\ \mu$m, $R_{\mathrm{ext}} = 1.25\ \mu$m (dot-dashed). At resonance the emitted energy spectrum may exceed the Planck prediction for a body much larger than the wavelength of interest by almost one order of magnitude; the dashed line illustrates Planck's formula ($T = 1200$ K). In the inset we specify the dielectric coefficient of SiC used in the simulation.

such as a half-infinite waveguide of rectangular cross section ($a_x \times a_y$). Based on a simple image-charge argument, one should not expect, in the first example, an enhancement of more than a factor of 2 in the emitted power. If a larger enhancement is required, it would be necessary to employ an infinite series of image charges as is the case in the second example.

The first case, of a dipole above an ideal metallic plane, is illustrated in the inset of Fig. 6 (top). The emitted power compared to that in free space is different for *perpendicular* and *parallel* dipoles:

$$P_z = P_{\rm FS}\left[3\int_0^{\pi/2} d\theta \sin^3\theta \cos^2\left(\frac{\omega}{c}h\cos\theta\right)\right], \quad (20)$$

$$\begin{pmatrix} P_x \\ P_y \end{pmatrix} = P_{\rm FS}\frac{3}{2\pi}\int_0^{\pi} d\phi \int_0^{\pi} d\theta \sin^3\theta \sin^2\left[\frac{\omega}{c}h\sin\theta\begin{pmatrix}\cos\phi \\ \sin\phi\end{pmatrix}\right]. \quad (21)$$

Obviously, the field components on the dipole are not identical; therefore, the emitted energy is

$$\begin{aligned}\varepsilon_0\langle E^2\rangle &= \varepsilon_0\left(\langle E_x^2\rangle + \langle E_y^2\rangle + \langle E_z^2\rangle\right)\\ &= \frac{1}{\pi^2 c^3}\int_0^\infty d\omega\omega^2\mathcal{E}(\omega,T)\\ &\quad\times\left[\frac{1}{2\pi}\int_0^\pi d\phi\int_0^\pi d\theta\sin^3\theta\sin^2\left(\frac{\omega}{c}h\sin\theta\cos\phi\right)\right.\\ &\quad+\frac{1}{2\pi}\int_0^\pi d\phi\int_0^\pi d\theta\sin^3\theta\sin^2\left(\frac{\omega}{c}h\sin\theta\sin\phi\right)\\ &\quad\left.+\int_0^{\pi/2} d\theta\sin^3\theta\cos^2\left(\frac{\omega}{c}h\cos\theta\right)\right]. \quad (22)\end{aligned}$$

In Fig. 6 (top) we present the form factor $F(\omega) = F_x(\omega) + F_y(\omega) + F_z(\omega)$,

$$\begin{aligned}F_x(\omega) &\equiv \frac{1}{2\pi}\int_0^\pi d\phi\int_0^\pi d\theta\sin^3\theta\sin^2\left(\frac{\omega}{c}h\sin\theta\cos\phi\right),\\ F_y(\omega) &\equiv \frac{1}{2\pi}\int_0^\pi d\phi\int_0^\pi d\theta\sin^3\theta\sin^2\left(\frac{\omega}{c}h\sin\theta\sin\phi\right),\\ F_z(\omega) &\equiv \int_0^{\pi/2} d\theta\sin^3\theta\cos^2\left(\frac{\omega}{c}h\cos\theta\right). \end{aligned} \quad (23)$$

When the height h above the plane is very small compared to the wavelength, the parallel polarizations become zero, and the perpendicular polarization is doubled due to an image beneath the plane. As the height is enlarged, the dipole acts as a free-space dipole with the form factor converging to 1 and with all three polarities converging to a similar probability of $1/3$. However, this convergence is not monotonic and certain ratios of height to wavelength yield a form factor which is *greater than 1*.

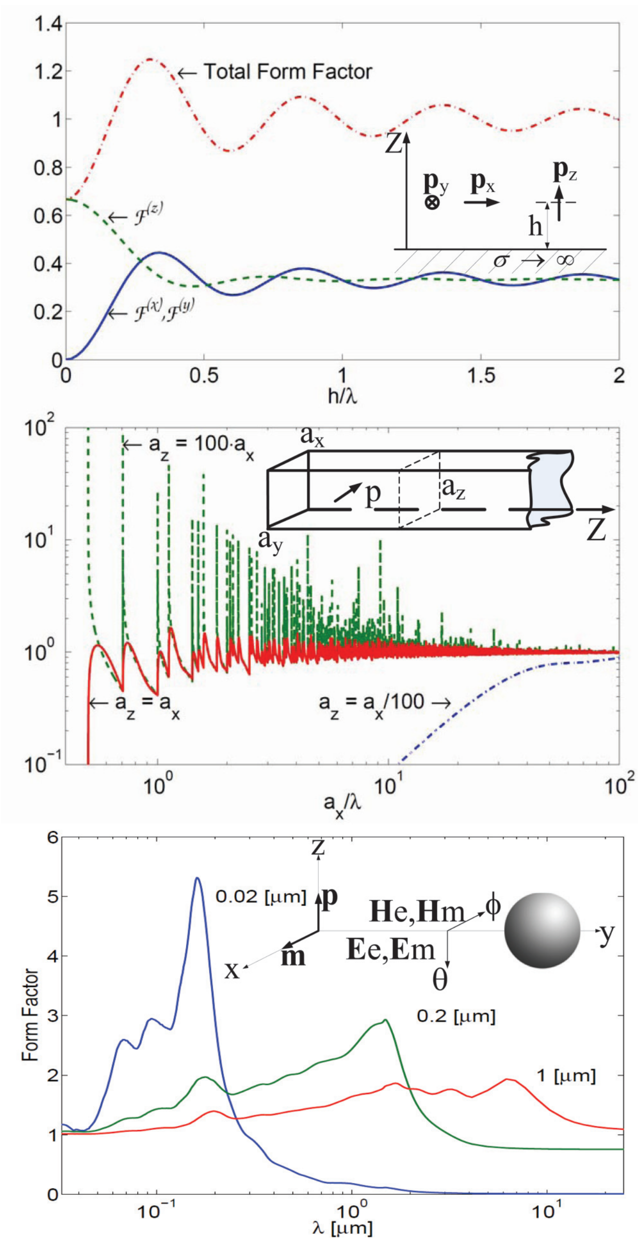

FIG. 6. (Color online) Top: Form factor of a dipole above an ideal plane as a function of its height normalized to the wavelength. A 20% enhancement is observed when $h/\lambda \sim 0.3$. Center: The radiation form factor for a uniform distribution of dipoles confined to the volume $a_x \times a_y \times a_z$ within a half infinite rectangular waveguide, as a function of the waveguide base normalized to the wavelength. For large a_z (dashed) the graph exhibits pronounced amplification of the thermal energy at $\lambda \sim a_x$. When $a_z = a_x$ (solid), there is a suppression of the first mode at $a_x = \lambda/2$. Bottom: Form factor of a tungsten sphere, for various radii: 0.02, 0.2, and 1 μm. For wavelengths shorter than the radius the form factor converges to unity. For wavelengths comparable with the radius the resonant character of the form factor is clearly revealed.

A second example is that of a blackbody confined in an ideal semi-infinite waveguide. First we consider a single dipole, then a gas of such dipoles ($\varepsilon_r \sim 1$) confined to $0 \leqslant z \leqslant a_z$. The geometry of the problem is detailed in the inset of Fig. 6 (center). Separating the problem into the longitudinal and transverse directions we arrive at the form factors

$$\begin{aligned} F_x(\omega) &= \frac{24\pi}{a_x a_y}\frac{1}{k^3}\sum_{\substack{n_x=0\\n_y=1}}^{k_\perp<k}\frac{k^2-k_y^2}{k_z}\cos^2(k_x b_x)\sin^2(k_y b_y)\sin^2(k_z b_z)\,g_{n_x},\\ F_y(\omega) &= \frac{24\pi}{a_x a_y}\frac{1}{k^3}\sum_{\substack{n_x=1\\n_y=0}}^{k_\perp<k}\frac{k^2-k_y^2}{k_z}\sin^2(k_x b_x)\cos^2(k_y b_y)\sin^2(k_z b_z)g_{n_y},\\ F_z(\omega) &= \frac{P_z}{P_{FS}} = \frac{24\pi}{a_x a_y}\frac{1}{k^3}\sum_{\substack{n_x=1\\n_y=1}}^{k_\perp<k}\frac{k_\perp^2}{k_z}\sin^2(k_x b_x)\sin^2(k_y b_y)\cos^2(k_z b_z),\\ k_x &= \frac{\pi n_x}{a_x},\quad k_y=\frac{\pi n_y}{a_y},\quad k_\perp=\sqrt{k_x^2+k_y^2},\quad k=\frac{\omega}{c},\quad k_z=\sqrt{k^2-k_\perp^2}, \end{aligned} \tag{24}$$

where $g_{n=0}=1/2$ and $g_{n\neq 0}=1$. Thus the radiated power is

$$\varepsilon_0\langle E^2_{(x,y,z)}\rangle = \frac{1}{3\pi^2c^3}\int_0^\infty d\omega\omega^2\Theta(\omega,T)F_{(x,y,z)}(\omega). \tag{25}$$

Rather than a single dipole we consider a uniform distribution of independent dipoles filling the waveguide, $0\leqslant z\leqslant a_z$. We therefore average (25) over all possible locations (b_x,b_y,b_z):

$$\begin{aligned} \varepsilon_0\langle E_x^2\rangle &= \frac{1}{\pi^2c^3}\int_0^\infty d\omega\omega^2\Theta(\omega,T)\frac{\pi}{a_x a_y}\frac{1}{k^3}\sum_{\substack{n_x=0\\n_y=1}}^{k_\perp<k}\frac{k^2-k_x^2}{k_z}[1-\mathrm{sinc}\,(2k_z a_z)],\\ \varepsilon_0\langle E_y^2\rangle &= \frac{1}{\pi^2c^3}\int_0^\infty d\omega\omega^2\Theta(\omega,T)_x\frac{\pi}{a_x a_y}\frac{1}{k^3}\sum_{\substack{n_x=1\\n_y=0}}^{k_\perp<k}\frac{k^2-k_y^2}{k_z}[1-\mathrm{sinc}\,(2k_z a_z)],\\ \varepsilon_0\langle E_z^2\rangle &= \frac{1}{\pi^2c^3}\int_0^\infty d\omega\omega^2\Theta(\omega,T)\frac{\pi}{a_x a_y}\frac{1}{k^3}\sum_{\substack{n_x=1\\n_y=1}}^{k_\perp<k}\frac{k_x^2+k_y^2}{k_z}[1-\mathrm{sinc}\,(2k_z a_z)]. \end{aligned} \tag{26}$$

In Fig. 6 (center) we plot the total form factor obtained from $F(\omega)=F_x(\omega)+F_y(\omega)+F_z(\omega)$. When a_z is large compared to the wavelength, the graph exhibits pronounced enhancement of the thermal energy at $\lambda\sim a_x$. With a smaller a_z, not only are the parallel polarizations suppressed, but also the perpendicular polarization of long wavelengths, resulting in thermal radiation limited to wavelengths which are much shorter than a_z.

To conclude this section, we presented the FDT and its relevance to Planck's BBR formula. We have shown that the radiation resistance of a dipole in various configurations may exceed that of a dipole in free space and, consequently, an enhancement of the radiated energy is possible also in *open structures*.

IV. RADIATION FROM SURFACES

Originally the FDT was developed for discrete components. In Ref. [20] Rytov (see also Landau and Lifshitz [19]) generalized the approach to distributed systems. Before we discuss the relevance to our goals, it is warranted to review the essentials of his theory: Given a force field $f(t,\vec r)$, it is assumed that it creates a reaction field $\xi(t,\vec r)$ within a volume V. Assuming a linear system this reaction is related to the force via a linear operator $\xi(\omega,\vec r)=\hat A f(\omega,\vec r)$. When no force is applied, a reaction field exists due to thermal fluctuations; hence the associated force is $f(\omega,\vec r)=\hat A^{-1}\xi(\omega,\vec r)$. Along similar lines to Callen and Welton's FDT, the spectral-spectral density of the correlation between the forces is shown to be

$$\begin{aligned} &\langle f^{(j)}(\omega,\vec r)f^{(k)*}(\omega',\vec r')\rangle_\omega\\ &\quad= \frac{j\mathcal{E}(\omega,T)}{2\pi\omega}\left(\hat A^{-1}_{jk}-\hat A^{-1*}_{kj}\right)\delta(\vec r-\vec r')\delta(\omega-\omega'), \end{aligned} \tag{27}$$

where j and k are any two components of the field. This formulation, relevant for a general field, may be applied to an electromagnetic field consisting of a six-component "displacement" ($\xi=\{\vec E,\vec H\}$) due to a six-component associated force $f=\{\vec{\mathfrak{D}},\vec{\mathfrak{B}}\}$ of electric and magnetic induction. Obviously, Maxwell's equations form the linear operator which relates these two quantities. The correlation of these forces is given by (27).

The major contribution of Rytov lies in replacing the external forces with currents and applying the *reciprocity theorem*, thus arriving at an expression of the radiated electromagnetic fields. Essentially the reciprocity theorem enables us to study the impact of Callen and Welton's dipoles oscillating within the material on the surrounding environment. Explicitly, we may denote the currents associated with the *external* electric displacement and magnetic induction as $\vec{j}_e = j\omega\vec{\mathfrak{D}}$ and $\vec{j}_m = j\omega\vec{\mathfrak{B}}$. We further denote the field components associated with the thermal fluctuation field within the body with the superscript "(th)", the location of the electric (magnetic) dipole by $\vec{r}_e$ ($\vec{r}_m$); the direction of the electric (magnetic) dipole is along a constant unit vector $\hat{n}_e$ ($\hat{n}_m$) and thus

$$\begin{aligned}\left\langle E^{(\mathrm{th})}_{n_e}(\vec{r}_e)H^{(\mathrm{th})*}_{n_m}(\vec{r}_m)\right\rangle_\omega &= \frac{1}{(j\omega p)(j\omega m)}\frac{\omega}{\pi}\mathcal{E}(\omega,T)\\ &\times\sum_\alpha\int_V d^3r\{\varepsilon'' E^{(\mathrm{e})}_\alpha(\vec{r},\vec{r}_e)E^{(m)*}_\alpha(\vec{r},\vec{r}_m)\\ &+\mu'' H^{(e)}_\alpha(\vec{r},\vec{r}_e)H^{(m)*}_\alpha(\vec{r},\vec{r}_m)\}\delta_\omega.\end{aligned} \tag{28}$$

The right-hand side determines the *normalized mixed* losses. "Mixed" in this context refers to the fact that (28) includes the vector product of two fields generated by two distinct sources and it is "normalized" since (28) includes the external source in the denominator, or explicitly

$$\begin{aligned}Q_{em}(\omega,\vec{r}_e,\vec{r}_m) &= \frac{2\omega}{(j\omega p)(j\omega m)}\\ &\times\int_V\left[\frac{\varepsilon''}{4}\vec{E}^{(e)}(\omega,\vec{r},\vec{r}_e)\cdot\vec{E}^{(m)*}(\omega,\vec{r},\vec{r}_m)\right.\\ &\left.+\frac{\mu''}{4}\vec{H}^{(e)}(\omega,\vec{r},\vec{r}_e)\cdot\vec{H}^{(m)*}(\omega,\vec{r},\vec{r}_m)\right]d^3r.\end{aligned} \tag{29}$$

Here the mixed losses are annotated with an index referring to the source dipoles. Thus the variance of the thermal spontaneous electromagnetic fields in (28) is a function of the induced losses of forced dipoles. Similarly, the covariances of the E and H spectral-spectral densities are

$$\begin{aligned}\left\langle E^{(\mathrm{th})}_{n_e}(\omega,\vec{r}_e)H^{(\mathrm{th})*}_{n_m}(\omega,\vec{r}_m)\right\rangle_\omega &= -\frac{2}{\pi}\mathcal{E}(\omega,T)\,Q_{em}(\omega,\vec{r}_e,\vec{r}_m),\\ \left\langle E^{(\mathrm{th})}_{n_e}(\omega,\vec{r}_e)E^{(\mathrm{th})*}_{n_m}(\omega,\vec{r}_m)\right\rangle_\omega &= \frac{2}{\pi}\mathcal{E}(\omega,T)\,Q_{ee}(\omega,\vec{r}_e,\vec{r}_m),\\ \left\langle H^{(\mathrm{th})}_{n_e}(\omega,\vec{r}_e)H^{(\mathrm{th})*}_{n_m}(\omega,\vec{r}_m)\right\rangle_\omega &= \frac{2}{\pi}\mathcal{E}(\omega,T)\,Q_{mm}(\omega,\vec{r}_e,\vec{r}_m),\\ \left\langle\left|E^{(\mathrm{th})}_{n_e}(\omega,\vec{r})\right|^2\right\rangle_\omega &= \frac{2}{\pi}\mathcal{E}(\omega,T)\,Q_{ee}(\omega,\vec{r}),\\ \left\langle\left|H^{(\mathrm{th})}_{n_m}(\omega,\vec{r})\right|^2\right\rangle_\omega &= \frac{2}{\pi}\mathcal{E}(\omega,T)\,Q_{mm}(\omega,\vec{r}).\end{aligned} \tag{30}$$

One must notice the difference in the roles of the dipole in Callen and Welton's and Rytov's formulations. In Callen and Welton's formulation, the dipole is the actual source of radiation within the body, for which one must find the radiation impedance of the surroundings. In Rytov's case, the dipole is located outside the BB, at the measurement location, and it generates a test signal, from which one may assess the radiation absorption. Once the various field components due to the unit dipole are established, one may determine the losses (Q) and through them the radial Poynting vector,

$$\begin{aligned}S^{(\mathrm{th})}_r(\omega,\vec{r}) &= \frac{1}{2}\left\langle E^{(\mathrm{th})}_\theta(\omega,\vec{r})H^{(\mathrm{th})*}_\phi(\omega,\vec{r})\right.\\ &\left.- E^{(\mathrm{th})}_\phi(\omega,\vec{r})H^{(\mathrm{th})*}_\theta(\omega,\vec{r})\right\rangle_\omega\\ &= \frac{1}{\pi}\mathcal{E}(\omega,T)\,[Q_{em}(\omega,\vec{r},\hat{n}_e=\theta,\hat{n}_m=\phi)\\ &- Q_{em}(\omega,\vec{r},\hat{n}_e=\phi,\hat{n}_m=\theta)].\end{aligned} \tag{31}$$

It is most important to realize based on the definition of the normalized mixed loss that a body will radiate *only* if it has losses.

As an example of emission from surfaces, let us consider a sphere of radius a made of tungsten. Our purpose will be to examine how the radiation spectrum of a classical (large) sphere changes as we reduce the sphere's radius. Due to symmetry, the fluctuations of the fields in both vertical and horizontal polarizations will be equal; thus (31) reduces to

$$S_r(\omega,\vec{r}) = \frac{2}{\pi}\mathcal{E}(\omega,T)\,Q_{em}(\omega,\vec{r},\hat{n}_e=\theta,\hat{n}_m=\phi). \tag{32}$$

Consequently, the form factor we are looking for is

$$F(\omega,a) = \frac{S_r(\omega,\vec{r},a)}{S_r(\omega,\vec{r},a_\infty)} = \frac{Q_{em}(\omega,\vec{r},\hat{n}_e=\theta,\hat{n}_m=\phi,a)}{Q_{em}(\omega,\vec{r},\hat{n}_e=\theta,\hat{n}_m=\phi,a_\infty)}, \tag{33}$$

where a is the variable radius of the sphere, and the radiation is normalized by a sphere of radius $a_\infty \gg a$. For simplicity's sake, we consider only dielectric loss ($\mu''=0$) and we assume that the dielectric properties of the material do not change, even when the radius of the sphere is taken to be very small.

When the test dipoles are placed as in the inset of Fig. 6 (bottom), the form factor reduces to the normalized absorption cross section $\bar{\sigma}_{\mathrm{abs}} = \sigma_{\mathrm{abs}}/\pi a^2$ of Mie scattering [[16], Sec. 4.4]. It is well known that $\bar{\sigma}_{\mathrm{abs}}$ can be greater than unity; therefore it is straightforward that the thermal radiation should be greater than the value obtained by the classical derivation, which accounts only for the geometrical area. In our simulations we used (spherical) functions from Ref. [55] and refractive index data for tungsten from Ref. [56]. We take a series of spheres with varying radii, starting at 10 nm and normalized by a sphere of 1 cm radius. The smallest radius is chosen to be two orders of magnitude larger than 1 Å so as to ensure the validity of the use of the dielectric coefficient. In Fig. 6 (bottom) we see that the form factor converges to 1, over all frequencies, as the radius grows. At small radii the form factor is larger than unity, indicating geometric enhancement when the radius is of the order of the wavelength ($\lambda \sim 2\pi a$).

With this example in mind, it is appropriate now to discuss Chow's study [2], which essentially concludes that the energy density in a closed cavity may exceed the value predicted by PF, but the energy emitted by an open structure cannot exceed the value predicted by PF. For this purpose, he considers a resonator consisting of lossless dielectric layers. In these layers he indeed shows that the energy may exceed the PF value. Once these layers are coupled to an extended, but limited, void which was chosen to represent the free-space region, he shows that the energy coupled into this region is always lower than predicted by PF. From the purely electromagnetic perspective, it is crystal clear that this configuration cannot represent an open structure (different boundary conditions), since at thermal equilibrium this represents a standing-wave configuration corresponding to a *large* cavity. It is well known that by incorporating in a large cavity any filter (e.g., dielectric layers), the modes' excitation is, at the best, reduced. Therefore, the amount of energy is always smaller than Planck's limit. In other words, the simulation result is believed to be correct but the conclusion drawn is not relevant for an open structure.

V. DISCUSSION

In this work we considered blackbody and thermal radiation for structures of size comparable with the radiation wavelength. Here we summarize the main conclusions of this study but also include some points of common knowledge (nos. 1 and 2) for completeness:

(1) Planck's formula is not valid for wavelengths larger than the size of the blackbody since the energy is identically zero.

(2) For frequencies slightly above the cutoff, the stored energy is not zero but the spectrum is discrete and therefore the PF is only a rough estimate.

(3) PF is an accurate description of the emitted or stored electromagnetic energy provided the wavelength is much shorter than the local radius of curvature of the BB. In other words, the wavelength is shorter than all three dimensions of the cavity.

(4) When in one dimension (thin film) or two dimensions (rod) the geometry is comparable to the wavelength, we developed an *analytic* expression that relates the energy density with the temperature, volume, and surface of the cavity.

(5) In a limited spectrum the geometrical enhancement of the emitted or stored energy may be orders of magnitude higher than predicted by the formula. Inherently, the Stefan-Boltzmann law is only weakly affected by the geometry—by less than one order of magnitude.

(6) The geometric enhancement occurs both in closed and in open structures.

(7) The fluctuation-dissipation theorem in its discrete form (Callen and Welton) or in its distributed form (Rytov) is the natural way to describe the thermal radiation emitted by an open structure.

Finally, an experiment we performed supports our theoretical conclusions. In the remainder of this section we describe its essentials. Its goal was to demonstrate that in a narrow frequency range, thermal radiation may exceed the value predicted by PF. A set of perforated Si wafers polished with an accuracy of 1 nm was examined. The geometry is revealed by two scanning electron microscope (SEM) pictures in the left frames of Fig. 7. It consists of 300-nm-diameter voids with a similar height and a pitch of 600 nm. Due to the relatively high loss, no electromagnetic coupling between the voids is expected and thus no collective effects are anticipated; in other words, each void acts as a separate resonator.

After being inserted in a furnace, the wafer was gradually warmed up to about 900 °C and the thermal radiation emitted was measured by a spectrometer (CI Systems SR-5000) located about 3 m away. Prior to measurements the spectrometer

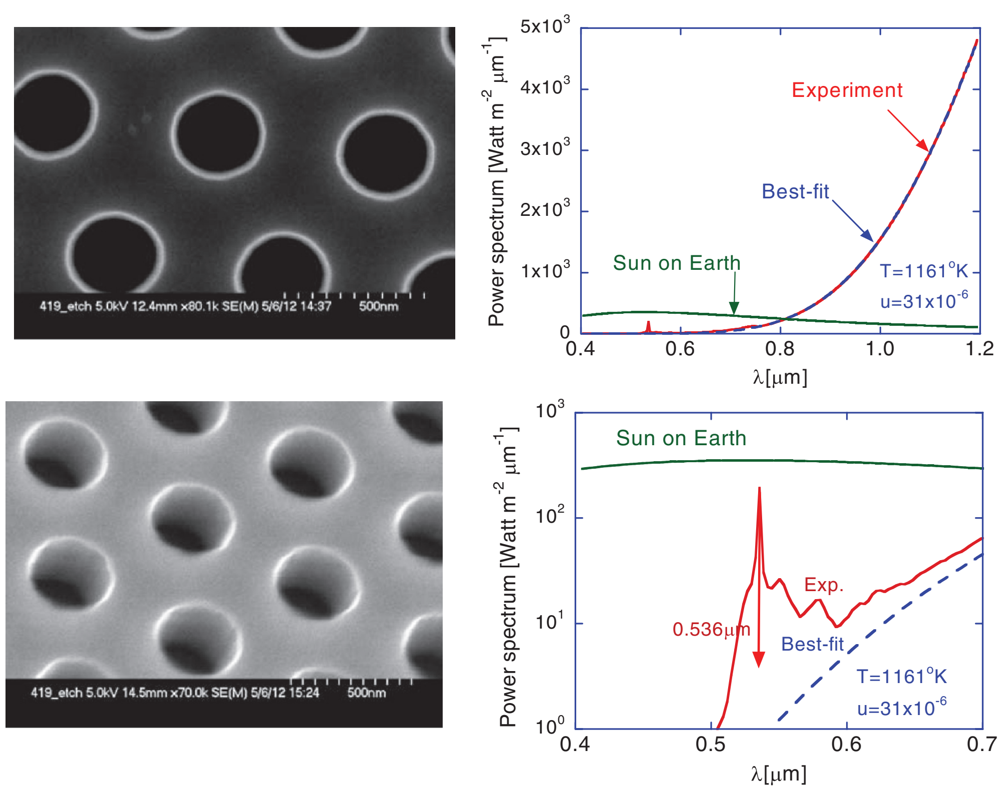

FIG. 7. (Color online) Left column: SEM picture of the emitting surface. Cylindrical voids (cavities) of 300 nm diameter and a similar height, and 600 nm pitch. Right column: Energy-flux spectrum (top) as extrapolated to the surface of the blackbody (solid) and a best fit to Planck's blackbody formula (dashed). Bottom: A zoom-in of the range between 0.4 and 0.7 μm. It clearly shows that there is a significant emission enhancement. As a reference, we plot the sun's energy flux spectrum as measured on earth.

was calibrated with a standard blackbody. In the top right frame of Fig. 7, the solid curve illustrates the experimental data for the energy flux spectrum as extrapolated to the surface of the blackbody. The dashed curve is a best fit to Planck's formula for the energy flux $S(\lambda,T)d\lambda = cu(\omega,T)d\omega$. For the range between 0.4 and 1.2 μm we found that the effective temperature is $T_{\rm expt} = 1161$ K and $\nu_{\rm expt} = 31.5 \times 10^{-6}$; these two parameters minimize the functional $\sum_i [S_i - \nu S(\lambda_i,T)]^2$ or explicitly $\nu_{\rm expt} = \langle S(\lambda_j,T)S_j\rangle_j / \langle S(\lambda_j,T)^2\rangle_j$ whereas

$$T_{\rm expt} = \min\left\{\sum_i [S_i - \langle S(\lambda_j,T)S_j\rangle_j \langle S(\lambda_j,T)^2\rangle_j^{-1} S(\lambda_i,T)]^2\right\}.$$

Each data point (S_i) corresponds to the maximum value from a sample of 120 measurements at each wavelength; the wavelength resolution is 3 nm. Except at short wavelengths, the two curves are essentially indistinguishable.

The bottom right frame of Fig. 7 is a zoom-in of the range between 0.4 and 0.7 μm. It clearly shows that there is a significant emission enhancement in particular in the range where the radiation overlaps geometric resonances. The peak occurs at 0.536 μm and it is more than 200 times larger than the value predicted by Planck's formula at this wavelength and temperature. As a reference, we plot the sun's energy-flux spectrum as measured on earth. Clearly, if a similar enhancement can be achieved close to 0.7 μm then at $T_{\rm expt} = 1161$ K we can get at that wavelength much higher intensity than the sun delivers at sea level.

ACKNOWLEDGMENT

This study was supported by the Technion's energy program (GTEP) and by the Bi-National Science Foundation (BSF) US-Israel.

[1] M. U. Pralle *et al.*, Appl. Phys. Lett. **81**, 4685 (2002).
[2] W. W. Chow, Phys. Rev. A **73**, 13821 (2006).
[3] S. E. Han, Phys. Rev. B **80**, 155108 (2009).
[4] M. Ghebrebrhan *et al.*, Phys. Rev. A **83**, 033810 (2011).
[5] A. I. Liptuga and N. B. Shishkina, Infrared Phys. Technol. **44**, 85 (2003).
[6] C. F. Bohren and D. R. Huffman, *Absorption and Scattering of Light by Small Particles* (Wiley-Interscience, New York, 1983).
[7] M. Planck, *Introduction to Theoretical Physics*, *Vol. V: Theory of Heat* (Macmillan, London, 1949).
[8] R. Courant and D. Hilbert, *Methods of Mathematical Physics* (Wiley, New York, 1989), Chap. VI, Sec. 4.
[9] S. M. Rytov, *Theory of Electric Fluctuations and Thermal Radiation* (Air Force Cambridge Research Center, Bedford, 1959).
[10] A. Einstein, Phys. Z. **18**, 121 (1917); also in *The Collected Papers of Albert Einstein* (Princeton University Press, Princeton, NJ, 1987).
[11] H. Weyl, Math. Ann. **71**, 441 (1912).
[12] T. Carleman, in *Proceedings of the Eighth Scandinavian Mathematics Congress, Stockholm* (Ohlsson, Lund, 1935), p. 34.
[13] Å. Pleijel, Commun. Pure Appl. Math. **3**, 1 (1950).
[14] F. H. Brownell, Pacific J. Math. **5**, 483 (1955).
[15] H. P. Baltes and E. R. Hilf, *Spectra of Finite Systems* (Bibliographisches Institut, Mannheim, 1976).
[16] A. Garcia-Garcia, Phys. Rev. A **78**, 023806 (2008).
[17] F. Reif, *Fundamentals of Statistical and Thermal Physics* (McGraw-Hill, New York, 1965).
[18] H. B. Callen and T. A. Welton, Phys. Rev. **83**, 34 (1951).
[19] L. D. Landau and E. M. Lifshits, *Statistical Physics* (Pergamon, Oxford, 1958).
[20] S. M. Rytov, Y. A. Kravtsov, and V. I. Tatarskii, *Principles of Statistical Radiophysics*, *Vol 3: Elements of Random Fields* (Springer-Verlag, Berlin, 1989).
[21] L. Mandel and E. Wolf, *Optical Coherence and Quantum Optics / Leonard Mandel and Emil Wolf* (Cambridge University Press, Cambridge, 1995).
[22] E. Wolf and D. F. V. James, Rep. Prog. Phys. **59**, 771 (1996).
[23] D. C. Bertilone, J. Mod. Opt. **43**, 207 (1996).
[24] D. C. Bertilone, J. Opt. Soc. Am. A **14**, 693 (1997).
[25] J. Le Gall, M. Olivier, and J. Greffet, Phys. Rev. B **55**, 10105 (1997).
[26] R. Carminati and J. Greffet, Phys. Rev. Lett. **82**, 1660 (1999).
[27] A. V. Shchegrov, K. Joulain, R. Carminati, and J. Greffet, Phys. Rev. Lett. **85**, 1548 (2000).
[28] C. Henkel, K. Joulain, R. Carminati, and J. Greffet, Opt. Commun. **186**, 57 (2000).
[29] J. Greffet *et al.*, Nature (London) **416**, 61 (2002).
[30] J. Greffet *et al.*, in *Optical Nanotechnologies. Manipulation of Surface and Local Plasmons*, edited by J. Tominaga and D. P. Tsai (Springer-Verlag, Berlin, 2003), pp. 163–182.
[31] A. Narayanaswamy and G. Chen, Appl. Phys. Lett. **82**, 3544 (2003).
[32] L. Hu, A. Narayanaswamy, X. Chen, and G. Chen, Appl. Phys. Lett. **92**, 133106 (2008).
[33] A. Narayanaswamy, S. Shen, L. Hu, X. Chen, and G. Chen, Appl. Phys. A: Mater. Sci. Process. **96**, 357 (2009).
[34] Y. Chen and Z. M. Zhang, Opt. Commun. **269**, 411 (2007).
[35] E. Hasman *et al.*, in *Nanomanipulation with Light II*, edited by D. L. Andrews, Proceedings of the SPIE Vol. 6131 (SPIE, Bellingham, WA, 2006), p. 61310.
[36] N. Dahan *et al.*, J. Heat Transfer **130**, 112401 (2008).
[37] G. Biener, N. Dahan, A. Niv, V. Kleiner, and E. Hasman, Appl. Phys. Lett. **92**, 081913 (2008).
[38] L. Schachter, patent 20100276000, 2010.
[39] E. Rephaeli and S. Fan, Appl. Phys. Lett. **92**, 211107 (2008).
[40] E. Rephaeli and S. Fan, Opt. Express **17**, 15145 (2009).
[41] I. Čelanović, Doctoral thesis, MIT, 2006.
[42] I. Celanovic *et al.*, in *MRS Spring Meeting*, Vol. 1162 (Materials Research Society, Pittsburgh, 2009), pp. 1–9.
[43] S. E. Han and D. J. Norris, Phys. Rev. Lett. **104**, 043901 (2010).
[44] M. Maksimović and Z. Jakšić, Phys. Lett. A **342**, 497 (2005).
[45] A. M. Yaremko *et al.*, Europhys. Lett. **62**, 223 (2003).

[46] S. Y. Lin, J. Moreno, and J. G. Fleming, Appl. Phys. Lett. **83**, 380 (2003).

[47] C. Chao, C. Wu and C. Lin, in *Photonic Crystal Materials and Devices IV*, edited by A. Adibi, S.-Y. Lin, and A. Scherer (SPIE 6128, San Jose, CA, 2006).

[48] Cha-Hsin Chao and Ching-Fuh Lin, in *Proceedings of the Conference on Lasers and Electro-Optics Europe, Munich* (IEEE, Piscataway NJ, 2005), p. 581.

[49] T. Trupke, P. Wurfel, and M. A. Green, Appl. Phys. Lett. **84**, 1997 (2004).

[50] S. Y. Lin, J. Moreno, and J. G. Fleming, Appl. Phys. Lett. **84**, 1999 (2004).

[51] C. Luo, A. Narayanaswamy, G. Chen, and J. D. Joannopoulos, Phys. Rev. Lett. **93**, 213905 (2004).

[52] D. Polder and M. Van Hove, Phys. Rev. B **4**, 3303 (1971).

[53] F. Bloch and A. Nordsieck, Phys. Rev. **52**, 54 (1937).

[54] D. R. Yennie, S. C. Frautschi, and H. Suura, Ann. Phys. (N.Y.) **13**, 379 (1961).

[55] C. Mõtzler, MATLAB functions for Mie scattering and absorption, version 2 (Institute of Applied Physics, University of Bern, 2002).

[56] E. D. Palik, *Handbook of Optical Constants of Solids* (Academic Press, New York, 1985).